Available online at www.sciencedirect.com
SCIENCE DIRECT®
Journal of Solid State Chemistry 177 (2004) 3439–3447
JOURNAL OF SOLID STATE CHEMISTRY
http://elsevier.com/locate/jssc

Bridged amine-functionalized mesoporous organosilica materials from 1,2-bis(triethoxysilyl)ethane and bis[(3-trimethoxysilyl)propyl]amine

Mohammad A. Wahab, Il Kim, and Chang-Sik Ha*

Department of Polymer Science and Engineering, Pusan National University, 30 Changjon-dong, Kumjong-gu, Pusan 609-735, Republic of Korea

Received 25 December 2003; received in revised form 30 April 2004; accepted 26 May 2004

Available online 20 July 2004

Abstract

Amine-functionalized, organic/inorganic hybrid mesostructured organosilica (BAFMO) materials have been synthesized and characterized from two bridged silsesquioxane precursors, 1,2-bis(triethoxysilyl)ethane (BTESE) and bis[(3-trimethoxysilyl)propyl]amine (BTMSPA). Mole ratios of BTESE ranged from 0.05, 0.10, 0.125, to 0.175. The synthetic pathway involves employing cetyltrimethylammonium bromide as a template under basic conditions at room temperature. X-ray diffraction (XRD) and transmission electron microscopy (TEM) studies revealed that the resultant BAFMO materials possess mesocopically ordered, hexagonal symmetries and well-defined morphologies. However, the order was decreased as the amount of BTMSPA increased, in terms of the d_{100} spacings and the unit cell parameters on XRD as well as the TEM images. N_2 gas sorption experiments showed a gradual decrease in both the surface area, from 1075 to 688 m^2/g, and the pore volume, from 2.08 to 0.55 cm^3/g, on increasing the amount of BTMSPA. The organic functionalization was successfully determined by Fourier-transform infrared and ^{13}C CP MAS NMR spectroscopy. X-ray photoelectron spectroscopy and elemental analysis results also confirmed the presence of Si–C bond as well as amine functionalities in the solvent-extracted mesoporous organosilica materials.

Keywords: Mesoporous organosilicas; Bis(3-trimethoxysilyl)propylamine; Nitrogen isotherms; Hybrid mesoporous materials; Transmission electron microscope (TEM); XPS; NMR

1. Introduction

The most important recent innovation in the field of periodic mesoporous materials is undoubtedly the use of bridged silsesquioxane molecules as precursors for the synthesis of periodic mesoporous organosilicas (PMOs) or bifunctional PMOs [1–14]. Integrating organic chemistry with inorganic materials allows the preparation of fascinating new materials with applications that were not possible with the first-generation materials [7]. It has been found that the structural ingredients and order of the resultant porous materials are directly related to their ability to perform desired functions in a particular application [2–11,15–18].

The preparation and characterization of silsesqioxane materials containing different organic groups has been reported previously [19–24]. Usually, these materials are amorphous in nature and, hence, they do not contain pore structures. Unfortunately, not all silsesquioxane precursors can be used to prepare the porous materials because of the lack of structural rigidity in the organic portion of the silsesquioxane. Using a silsesquioxane featuring a flexible organic group results in a disordered material. For this reason, all mesoporous organosilicas reported to date contain aliphatic organic groups with relatively short chains (ethane, ethylene) or aromatic (arylene, thiophene) moieties [2,7,10,15]. Some very useful functional groups, including amines and thiols, have not been incorporated into PMOs on demand because of the lack of available precursors. For instance, the organic bridging moiety of bis[3-(trimethoxysilyl)-propyl]ethylenediamine (TMSEN) is too flexible to

*Corresponding author. Fax: +82-51-514-4331.
E-mail address: csha@pusan.ac.kr (C.-S. Ha).

0022-4596/$ - see front matter © 2004 Elsevier Inc. All rights reserved.
doi:10.1016/j.jssc.2004.05.062

"stand alone" after extraction; removal of the surfactant from the final mesoscopic composites of these monomers results in the collapse of the polymer matrix [25]. Very recently, TMSEN-containing porous materials were prepared—but with a loading as small as 5 mol%—under basic conditions and applied for the adsorption of metal ions, such as, Zi, Cu, and Ni [26]. Only a few studies have been undertaken using amino-terminated trialkoxysilanes to form amine-functionalized mesoporous materials; this functionalization pathway has been extended to the synthesis of PMOs containing ethylenediamine moieties for metal ion adsorption and the creation of PMOs containing various functional groups [6,8,9,15,26–30]. It has been suggested that preparing amine-functionalized materials with higher concentrations of functional groups will be important for enhancing their molecular accessibility in adsorbence and catalysis applications [27], because the viability of using amine-functionalized PMOs in applications involving adsorbed organic compounds or biomolecules may well depend on their loading levels as well as the nature of the porous structure of the organosilica materials. The effects that functional organosilanes have on their resultant materials have been discussed in terms of structural order [31–33]. Judicious choice of an alkyl chain, and its functional groups, to bridge between the two silica atoms could be a very useful technique for solving other ambitious problems. To the best of our knowledge, in this paper we describe the first use of bis[(3-trimethoxysilyl)propyl]amine (BTMSPA) and 1,2-bis(triethoxysilyl)ethane (BTESE) as co-precursors for producing amine-functionalized hybrid mesoporous materials under basic conditions.

2. Experimental

2.1. Materials and sample preparation

BTESE (96%), cetyltrimethylammonium bromide (CTAB), and BTMSPA (97%) were purchased from Sigma-Aldrich and were used as received. Ammonia water, hydrochloric acid (HCl), methanol, and deionized water were also used as received.

2.2. Syntheses of bridged amine-functionalized mesoporous organosilicas (BAFMO series)

We synthesized the bridged amine-functionalized mesostructured organosilica (BAFMO) materials by following our previously reported procedure [14]. For example, the mesoporous organosilica material BAFMO-0 was prepared by dissolving a mixture of BTESE/BTMSPA and CTAB (the mole ratio of (BTESE/BTMSPA): CTAB) is 2.29:1 in a mixture of water and ammonia water (6.56:1). The mixture was stirred vigorously for 2–3 h, during which time a white precipitate formed. After being aged for a few days at 80°C, the resultant mixture was washed with methanol/water and dried at atmospheric pressure.

2.3. Preparation of BAFMO series 1–4

The BAFMO analogs were prepared following the same procedure as that for BAFMO-0 above by simply altering the amount of BTESE in the BTESE/BTMSPA mixture. Thus, mixtures of $8.8x$ mmol of BTMSPA and $8.8(1-x)$ mmol of BTESE ($x = 0.05$, 0.10, 0.125, and 0.175) were used to synthesize the hybrid, amine-functionalized mesoporous materials BAFMO-1, BAFMO-2, BAFMO-3, and BAFMO-4, respectively. The mole fractions of BTESE are listed in Table 1. The approach to achieve mentioned series is to generate amine funcionalized mesoporous materials by inserting organic spacers into the silica network, as shown in Scheme 1.

2.4. Surfactant extraction

The surfactant (CTAB) was extracted from all of the hybrid samples using the following general procedure: The as-synthesized powder sample (0.5 g) was placed in a Soxhlet thimble and extracted with a mixture of conc. HCl (36%, 5 g) and methanol (150 g) whilst stirring for 12 h at 60°C. Subsequently, the extracted sample was

Table 1
Textural properties of solvent extracted amine functionalized hybrid BAFMO materials

Sample code	Mole fraction of BTESE(x)[a]	d_{100} (nm)	a_O[b] (nm)	Pore diameter (nm)	Surface area (m^2/g)	Pore volume (cm^3/g)
BAFMO-0	0	5.5	6.3	3.4	1071	2.08
BAFMO-1	0.05	5.5	6.3	3.5	970	0.84
BAFMO-2	0.10	5.0	5.8	3.0	759	0.56
BAFMO-3	0.125	4.4	5.1	3.3	750	0.61
BAFMO-4	0.175	4.3	5.0	3.0	688	0.55

[a] Mixtures of $8.8x$ mmol of BTMSPA and $8.8(1-x)$ mmol of BTESE ($x = 0.05$, 0.10, 0.125, and 0.175) were used to synthesize the hybrid, amine-functionalized mesoporous materials BAFMO-1, BAFMO-2, BAFMO-3, and BAFMO-4, respectively.

[b] $d_{100}/1.732$ (assuming hexagonal symmetry).

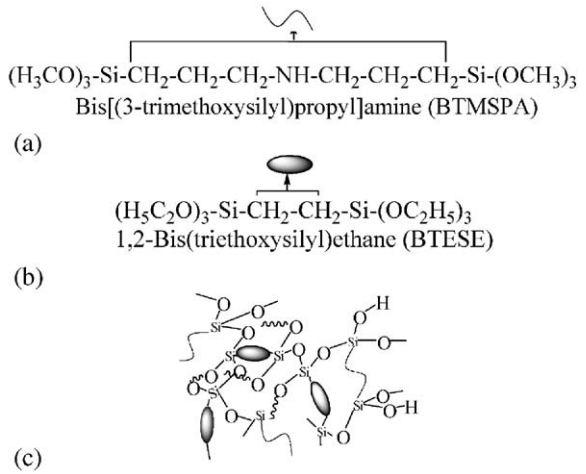

Scheme 1. Representative precursors (a and b) used in this work and probable network structure of hybrid poly(silsesquioxane) with organic bridging group (c).

washed with a copious amount of a mixture of water and methanol, and then dried in air.

2.5. Measurements and characterization

The formation of mesostructures of the hybrid BAFMO series was confirmed by their X-ray diffraction (XRD) patterns obtained on a Rigaku Miniflex (0.05 kV) instrument using a Cu$K\alpha$ radiation source with a 2θ step of 0.01° and a step time of 1 s. All samples were scanned under the same conditions ($2\theta = 0.7-5°$). The textural properties of the solvent-extracted BAFMO series were analyzed by recording the nitrogen adsorption/desorption isotherms according to the Brunaumer, Emmett and Teller method at 77 K on a Micromeretics ASAP2010 apparatus. The pore-size distributions were estimated from the desorption branch of the isotherm by the Barret–Joyner–Halenda (BJH) method. All the samples were dehydrated at 150°C for 24 h prior to nitrogen gas adsorption. Scanning electron microscopy (SEM; Hitachi S-4200) was used to observe the morphologies of some of the hybrid samples. Prior to measurement, the samples were mounted on a carrier made from glassy carbon and coated with a film of gold. Transmission electron microscopy (TEM) images were obtained using a JEOL JEM-2010 microscope operating at 200 kV. The sample for the TEM images was prepared by dispersing a large number of particles of the product in methanol by ultrasonication and then pouring the solution into a holey carbon grid. The removal of the surfactant and the presence of organic groups in the BAFMO series were confirmed by Fourier-transform infrared (FTIR) spectroscopy (React IR™ 1000, Applied System, ASi). The ^{13}C CP MAS NMR spectrum was obtained with a Bruker DSX400 spectrometer. The X-ray photoelectron spectroscopy was performed using a VG-Scientific ESCALAB 250 spectrometer equipped with a monochromated Al$K\alpha$ X-ray source. An energy of 0.05 eV was used for the narrow scan spectrum; 1 eV was used for the wide scan spectrum. Elemental analysis was conduced with an Elemental Analyzer (PA 206). Thermogravimetric analysis (TGA) was carried out using a Perkin–Elmer TGA 7 at a heating rate of 10°C/min under a nitrogen atmosphere.

3. Results and discussion

3.1. XRD patterns of bridged amine-functionalized mesoporous organosilicas (BAFMO series)

Fig. 1 depicts the XRD patterns for solvent-extracted mesostructures of the BAFMO series prepared from variable loadings of BTMSPA in the synthesis mixtures. These materials were prepared using BTMSPA/(BTMSPA + BTESE) molar ratios of 0.05, 0.10, 0.125, and 0.175. All of the samples exhibit one single peak in the low-angle Bragg diffraction, which indicates the characteristics of ordered materials. Similar "single reflection peak" has also been used for the mesoporous materials by earlier authors [14,34,35]. The absence of

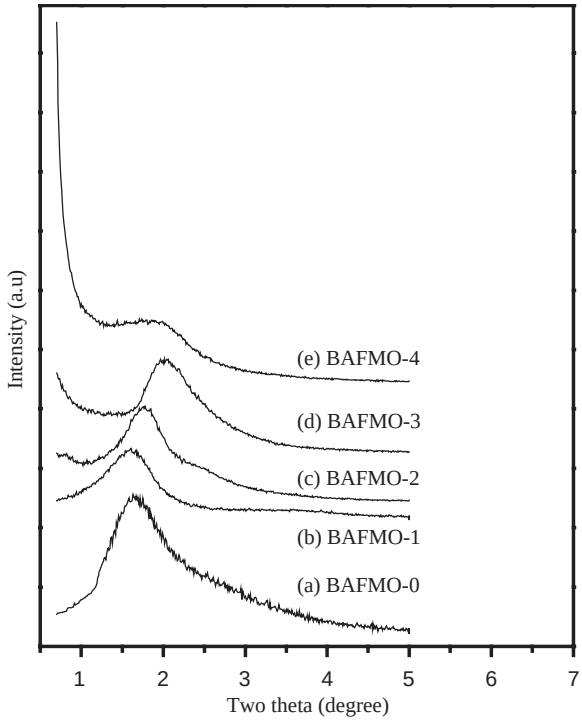

Fig. 1. XRD patterns of solvent-extracted BAFMO-series: (a) BAFMO-0, (b) BAFMO-1, (c) BAFMO-2, (d) BAFMO-3, and (e) BAFMO-4. The sample code, BAFMO-x, where x is 0–4, is referred to in Table 1. Mixtures of different ratios of BTMSPA and BTESE were used as co-precursors to synthesize bridged amine-functionalized, hybrid mesostructured organosilica (BAFMO) materials.

resolved higher-angle peaks indicates, however, that any structural order of the extracted hybrid materials does not extend over a long range. For the sake of comparison, an organosilica material was prepared from pure BTESE under the same conditions, but without the addition of BTMSPA to the synthesis mixture. The XRD pattern of this mesoporous organosilica (BAFMO-0) shows a single, low-Bragg-angle peak centered at $2\theta = 1.62°$, which corresponds to lattice spacing of 5.5 nm. Table 1 lists the d_{100} spacings for the BAFMO series. The XRD patterns indicate that the intensity of the d_{100} spacing reflection decreases and become broad as the loading of BTMSPA increases. Furthermore, when the mole ratio of BTMSPA/(BTMSPA + BTESE) is 0.175, the intensity of the d_{100} reflection is markedly decreased. This observation can be related to the highly amorphous nature of BTMSPA [33]. A similar trend has been reported for hybrid mesoporous materials formed using different precursors; it depends strongly on the nature of the organosilane that is incorporated for further organic functionalization [9,14,36–39]. Table 1 also indicates that the d_{100} spacings decrease from 5.50 nm (BAFMO-0) to 4.30 nm (BAFMO-3) as the amount of BTMSPA increases. Such a trend—the unit cell parameter decreasing as the loading of the organic groups increases—has been commonly observed for materials synthesized by the co-condensation of tetraethoxysilane or tetramethoxysilane and organosilanes [14,29,37,39]. Therefore, the decrease in the d spacings with increasing amounts of BTMSPA in the synthesis mixtures in the present series of materials indicates a concomitant increase in the loading of BTMSPA. Lim et al. [39], have demonstrated that the reduction in the d_{100} spacing reflections, as shown in Fig. 1, may be partially attributed to lower local order, such as variations in wall thickness. They also suggested that the reduction in the peak intensity occurs mostly because of contrast matching between the amorphous silicate framework and the organic moieties that are located in the walls of the channels. The BAFMO series showed features that agree with previously reported properties on organic-functionalized, hybrid mesoporous materials [14,29,36,37,40].

3.2. Scanning electron microscope and transmission electron microscope

Fig. 2 depicts SEM images of some amine-functionalized hybrid materials. The resultant hybrid materials form primary particles (diameter of ca. 0.6 μm for BAFMO-2 and BAFMO-3; 1.8 μm for BAFMO-4) that agglomerate to form clusters with particles in the range 0.6–1.8 μm. Higher-magnification images of the samples are also provided in Fig. 2 (indicated by arrows), which show clearly the features of the particles that have

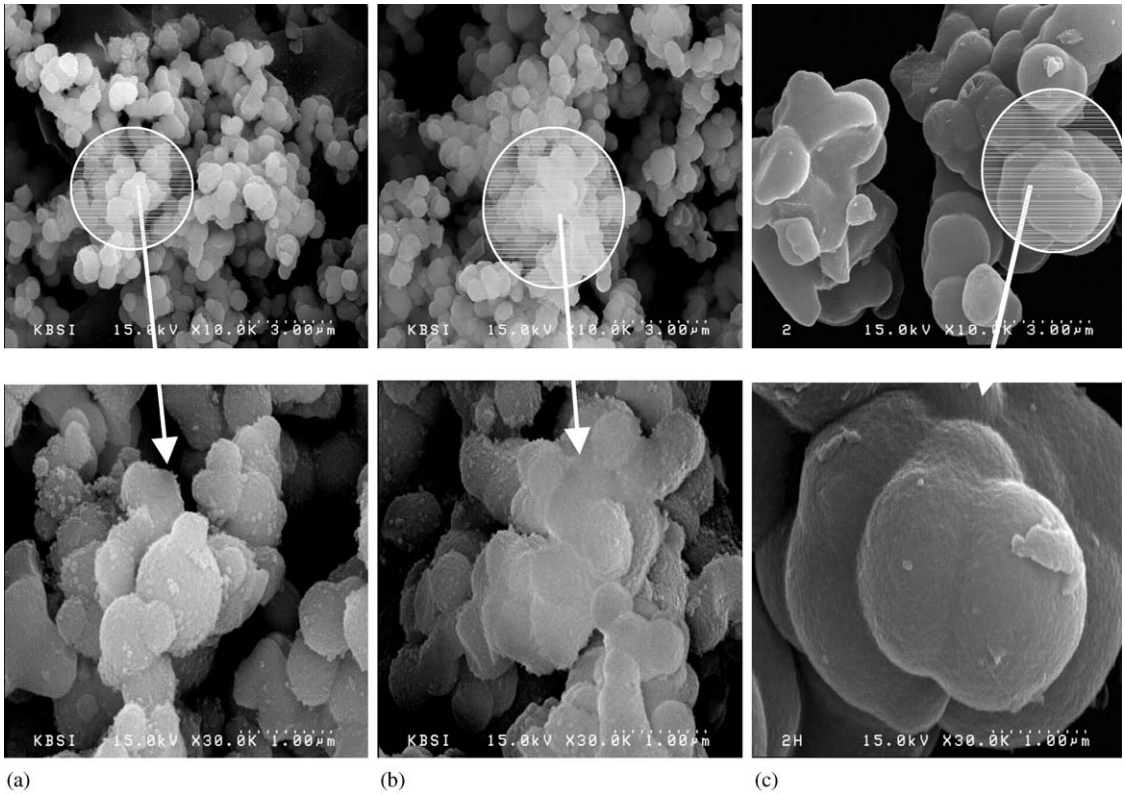

Fig. 2. SEM images of the solvent-extracted samples: (a) BAFMO-2, (b) BAFMO-3, and (c) BAFMO-4, where higher-magnification images of the samples are provided at the bottom for the portions indicated by arrows.

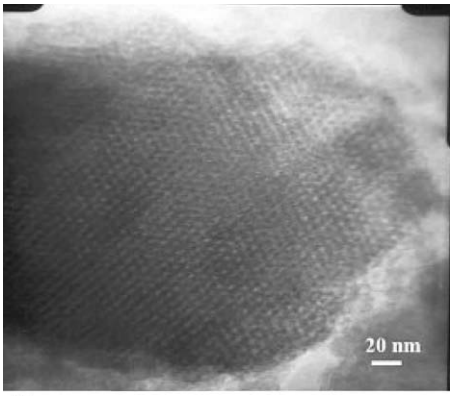

(a)

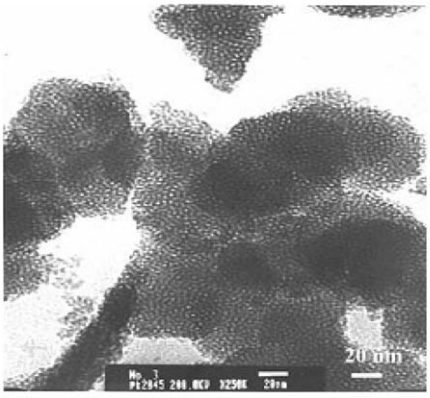

(b)

Fig. 3. TEM of the solvent-extracted BAFMO-2 (a), and BAFMO-3 (b).

agglomerated into clusters. Similar morphologies have been observed by SEM for other hybrid mesoporous materials [41]. Although the XRD reflections in Fig. 1 were not sufficient to identify unambiguously the exact types of structures of each of the samples reported herein, the TEM images obtained for BAFMO-2 (Fig. 3) provide direct evidence for the occurrence of hexagonal-type mesopores but BAFMO-3 consists of disordered worm-like mesopores. Fig. 3b indicates the TEM image for the BAFMO-3. These results are very similar to that of other previously reported bifunctional, hybrid mesoporous structures [14,37]. However, the TEM images for the BAFMO-2 and BAFMO-3 showed well consistent pore diameters with those obtained using desorption branch by the BJH method although BAFMO-3 possess rather disordered worm-like mesopores. The disorder results from the higher loading of BTMSPA effect on the surface area and pore volume of the resulting materials, as shown in Table 1.

3.3. Surface area, pore volume, and pore diameter

The results of the N_2-adsorption/desorption isotherms of the solvent-extracted hybrid BAFMO series and their corresponding pore-size distributions are presented in Figs. 4 and 5, respectively. BAFMO-0 shows a clear type-IV isotherm [42]. Indeed, we obtained type-IV isotherms for BAFMO-1 and BAFMO-2, which have the lowest loadings of BTMSPA, that are comparable to that obtained (Fig. 4) for the pristine BAFMO-0 sample. With higher loadings of BTMSPA, the isotherms show a tendency to change from type-IV to type-I. A similar trend observed in the appearance of isotherms is observed commonly for organic-functionalized hybrid materials with higher loading of organic groups [14,15,24,32,40]. In the current case, the degree of disordering increases with increased loadings of BTMPSA because of its highly amorphous nature [33]. Table 1 presents the textural properties of the BAFMO series. The surface areas for the materials in the BAFMO series systematically decrease with increased

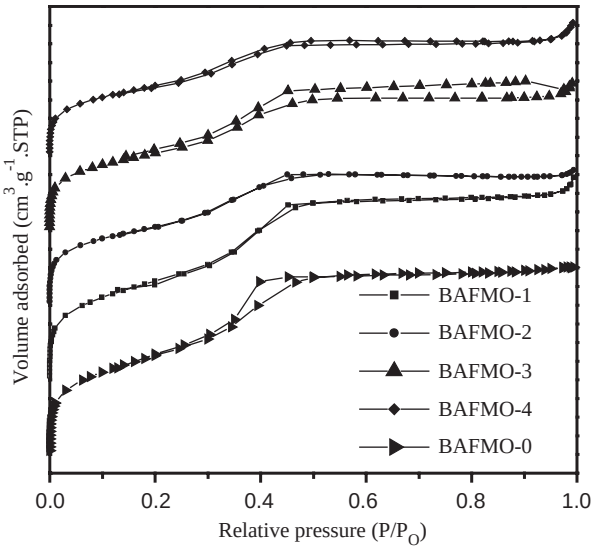

Fig. 4. N_2 isotherms of solvent-extracted hybrid BAFMO series.

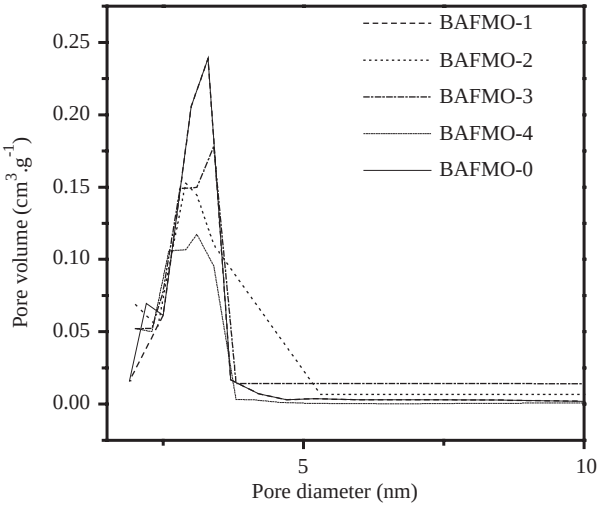

Fig. 5. Pore-size distribution of solvent-extracted hybrid BAFMO series.

loadings of BTMSPA, which suggests the functionalization with BTMSPA has occurred. These results in the present BAFMO series are strongly supported by the previously published reports on organic/inorganic hybrid mesoporous materials [14,15,26,27,36,40]. Table 1 indicates that the surface area and pore volume is decreased whereas pore size remains relatively unchanged. It is suggested that most of the BTMSPA anchored into outer surface of walls and led to the thinner wall. The reduction in surface area and pore volume results from disorder mesopores of the resulting materials due to higher loading of the BTMSPA.

3.4. Monitoring the removal of surfactant and the presence of organic groups by FTIR spectroscopy and ^{13}C CP MAS NMR spectroscopy

FTIR spectroscopy was used to detect the presence of organic groups in the as-synthesized and solvent-extracted samples (Fig. 6). The decrease in the intensity of the peak at 2927 cm^{-1} for the BAFMO-2 sample after solvent extraction indicates that the removal of surfactant from the final hybrid materials had occurred [14,43]. The FTIR spectra of the solvent-extracted BAFMO-2 reveals that the organic moieties remain intact—as verified by the presence of vibrations at 1423, 1270 and 1163 cm^{-1} along with those in the lower regions at 780 and 701 cm^{-1}—while the sharp peak at 1000–1100 cm^{-1} confirmed the formation of siloxane bonds [14,33,44,45]. The Si–O–H group shows a strong IR band involving Si–O stretching at 915 cm^{-1} [46]. Furthermore, the IR spectra strongly supports the presence of absorption bands that are attributable to N–H bonds (1645 and 3400 cm^{-1}) [10,15], while the relatively broad peaks at 780 and 1160 cm^{-1} indicate the presence of an N–H wagging vibration and the antisymmetrical stretch of a C–N–C moiety, respectively; a peak belonging to a secondary amine was also clearly visible at 695 cm^{-1} in each spectrum [10,15,33,44,45]. The IR spectra confirm that the organic moieties are linked co-valently to the silica framework in the final hybrid materials.

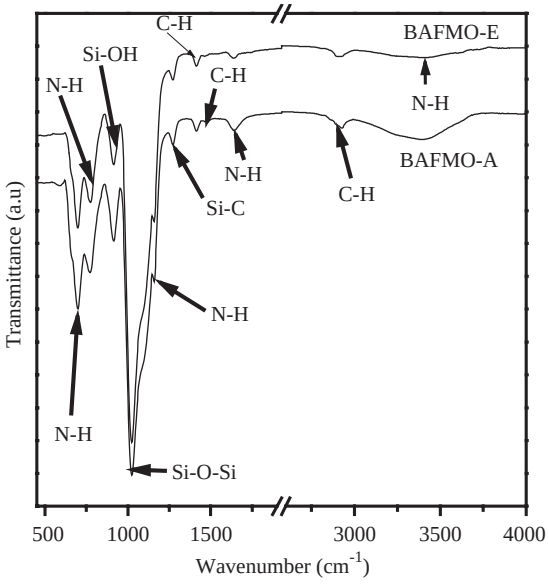

Fig. 6. FTIR spectra of BAFMO-2, where A and E are indicated for as-synthesized and solvent extraction sample.

The ^{13}C CP MAS NMR spectrum (Fig. 7) exhibits the most prominent peak at 5.83 ppm (carbon silicon bond) [9,12] and several sp^3 carbon atoms in the range of 10–55 ppm, which are characteristics of the organic fragments of BTMPSA in the solvent-extracted materials [47–53]. In particular, the spectrum of the BAFMO-2 consisted of three important peaks at 11.67, 23.01, and 42.63 ppm, corresponding to the C atoms of the ≡Si–CH_2–CH_2–CH_2–NH–CH_2–CH_2–CH_2–Si≡ group in sequence from left to right as indicated by number, supporting the BTMPSA functionalized mesoporous organosilica materials. The signal at 30.11 ppm can be attributed to the other two carbons (C1 and C2). The broad and very negligible chemical shift at 67–69 ppm supports the almost complete removal of surfactant by solvent extraction and very negligible amount of the unreacted ethoxy group is indicated by the presence of small shoulder peak at 19.25 ppm [12]. The broad peak at around 49 ppm is due to the trapped methanol in the solvent-extracted materials [9].

3.5. X-ray photoelectron spectroscopy (XPS) and elemental analysis

Fig. 8(a) shows the survey scan spectrum for the solvent-extracted BAFMO-2, which exhibits the presence of several peaks at binding energies of ca. 99.15, 282.69, 399.91, and 529.52 eV corresponding to Si 2*p*, C 1*s*, N 1*s*, and O 1*s*, respectively [54,55]. Particularly, it is

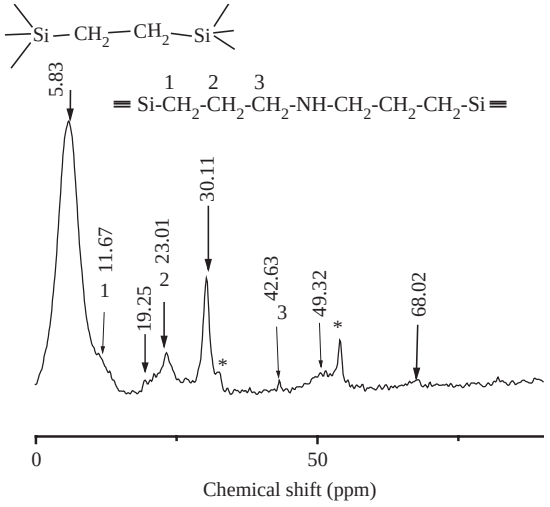

Fig. 7. ^{13}C CP MAS NMR spectrum of the solvent-extracted BAFMO-2.

noteworthy that the high-resolution N 1*s* spectrum in Fig. 8(b) indicates the presence of nitrogen atoms in the solvent-extracted materials, which also supports the BTMSPA functionalization in our mesoporous organosilica materials. Fig. 9 shows the high-resolution Si 2*p* spectra for the BAFMO-0 (a) and BAFMO-2 (b). The decrease in the Si 2*p* binding energy for the BTMSPA functionalized material (BAFMO-2) compared to the pristine BAFMO-0, strongly suggests a corresponding increase in number of secondary amine BTMSPA, i.e., there is an increase in number of nitrogen atoms around the pristine PMO materials. Asefa et al. [53] found similar results for the periodic mesoporous aminosilica materials, PMAs. They reported that the binding energy for the Si 2*p* core electrons decreases due to the increasing number of less electronegative atoms such as nitrogen into mesoprorous materials. Similar binding energy curves have also been reported for other porous materials [56].

Elemental analysis of the solvent-extracted BAFMO-2 was also performed. The total compositions of the sample were found to be 86.3%. The compositions of Si, O, C, H, and N are respectively 43.2%, 16%, 20%, 5%, and 1%, as expected. Among the total percentages, the amine group of the sample was calculated as 6%. Gaber and co-workers [15] reported similar low elemental analysis values for their amine-containing organosilane to prepare amine-functionalized mesoporous materials. Since the amine-containing trialkoxysilanes showed faster hydrolysis compared to the precursor BTESE, homocondensation would be likely to occur with more chances instead of co-condensation with BTESE. It was suggested, therefore, that they are unable to form the siloxane linkages necessary to incorporate them into the matrix, when the BTESE condenses around the micelle assemblies during the formation of the ordered mesocopic composite material [15,27]. The resulting clusters might be washed out of the composite material during the extraction process.

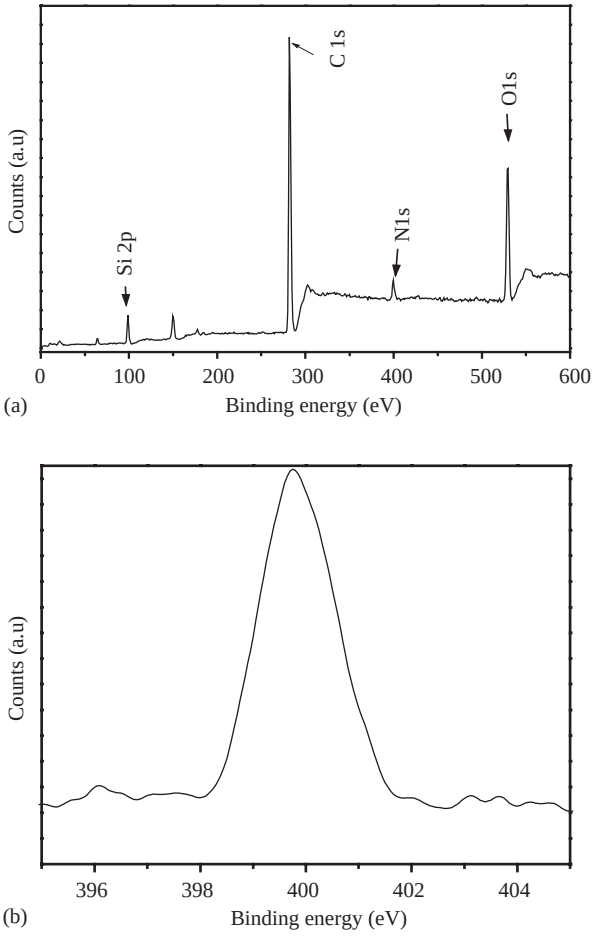

Fig. 8. (a) X-ray photoelectron survey scan spectrum for the solvent-extracted BAFMO-2. (b) High-resolution N 1*s* spectrum of the BAFMO-2 sample.

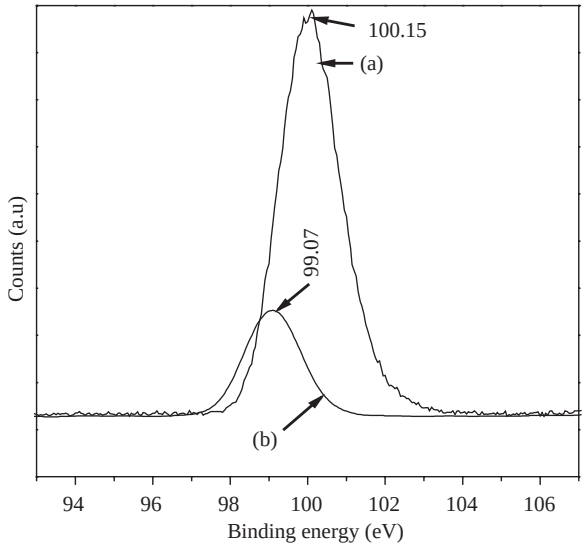

Fig. 9. High-resolution Si 2*p* spectra for BAFMO-0 (a), and BAFMO-2 (b).

3.6. Measuring weight loss by thermogravimetric analysis

TGA was performed on the as-synthesized and solvent-extracted sample BAFMO-2 under a nitrogen atmosphere. In Fig. 10, a significant weight loss of ca. 6.89% in the temperature range 125–350°C corresponds mainly to the thermal decomposition of the surfactant and possibly a negligible amount of the matrix of BTMSPA; we attribute the weight loss of ca. 36.72% found between 350°C and 700°C to the decomposition of the bridging organic groups. The solvent-extracted BAFMO-2 shows a moderate weight loss of ca. 13% in the temperature range 400–750°C, which is due to the loss of organic groups in the fragments [44]. Fig. 10 also confirms that CTAB is removed upon solvent extraction.

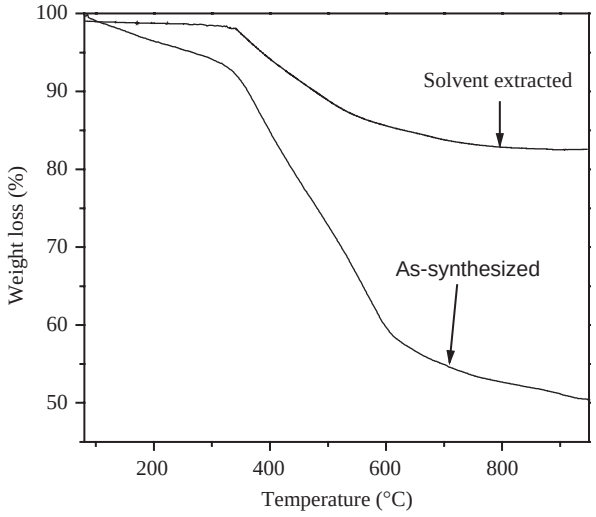

Fig. 10. The weight loss behaviors of the hybrid BAFMO-3.

4. Conclusions

We prepared amine-functionalized hybrid mesoporous materials by the co-condensation of bis(1,2-triethoxysilyl)ethane and BTMSPA, where the two bridged organic functions are introduced into the materials under basic conditions. We have outlined and explained the effects that the amount of BTMSPA in the synthetic mixture have on the structural and textural properties of these porous materials. Removal of the template was accomplished successfully by extracting with an acidic methanol/water mixture, and was verified with FTIR spectroscopy and TGA. XRD patterns suggest typical uniform mesoporous structures, and TEM images suggest hexagonally packed porous structures. This observation indicates that the porous structure in these mesoporous materials remains intact during extraction and that these materials exhibit sufficient structural rigidity under the conditions used. Based on the N_2 gas sorption experiments, when the amount of BTMSPA is increased, we observed a gradual decrease in both the surface area, from 1075 to 688 m^2/g, and the pore volume, from 2.08 to 0.55 cm^3/g. The hybrid materials exhibit a correlated relationship between the types of isotherms and the loadings of BTMSPA. The organic functionalization was successfully determined by FTIR and ^{13}C CP MAS NMR spectroscopy, respectively. XPS results also indicate the presence of nitrogen atoms in solvent-extracted materials and ultimately supports the formation of the BTMSPA-incorporated mesoporous organosilica materials. The results suggested that it is possible to introduce two bridged silsesquioxanes into the same mesoporous materials with higher loadings.

Acknowledgments

This work was supported by the National Research Laboratory Program, the Center for Integrated Molecular Systems, POSTECH, Korea, Pusan National Overseas Research Grant and the Brain Korea 21 Project. The authors are highly grateful to Professor R. Ryoo of KAIST for the XRD measurements.

References

[1] C.T. Kresge, M.E. Leonowicz, W.J. Roth, J.C. Vartuli, J.S. Beck, Nature 259 (1992) 710.
[2] S. Inagaki, S. Guan, Y. Fukushima, T. Ohsuna, O. Terasaki, J. Am. Chem. Soc. 121 (1999) 9611.
[3] Y. Goto, S. Inagaki, Chem. Commun. (2002) 2410.
[4] S. Guan, S. Inagaki, T. Ohsuna, O. Terasaki, J. Am. Chem. Soc. 122 (2000) 5660.
[5] M. Kruk, M. Jaroniec, S. Guan, S. Inagaki, J. Phys. Chem. B 105 (2001) 681.
[6] T. Asefa, M.J. McLacchlan, N. Coombs, G.A. Ozin, Nature 402 (1999) 867.
[7] C.Y. Ishii, T. Asefa, N. Coombs, M.J. MacLachlan, G.A. Ozin, Chem. Commun. (1999) 2539.
[8] O. Dag, C.Y. Ishii, T. Asefa, M.J. MacLachlan, H. Grondey, N. Coombs, G.A. Ozin, Adv. Func. Mater. 11 (2001) 213.
[9] B.J. Melde, B.T. Holland, C.F. Blanford, A. Stein, Chem. Mater. 11 (1999) 3302.
[10] S.R. Hall, C.E. Fowler, B. Lebeau, S. Mann, Chem. Commun. (1999) 201.
[11] O. Muth, C. Schellbach, M. Froba, Chem. Commun. (2001) 2032.
[12] W. Guo, J. Park, M. Oh, H. Jeong, W.J. Cho, I. Kim, C.S. Ha, Chem. Mater. 15 (2003) 2295.
[13] W. Guo, I. Kim, C.S. Ha, Chem. Commun. 15 (2003) 2692.
[14] M.A. Wahab, I. Kim, C.S. Ha, Micropor. Mesopor. Mater. 69 (2004) 19.
[15] M.C. Burleigh, M.A. Markowitz, M.S. Spector, B.P. Gaber, J. Phys. Chem. B 105 (2001) 9935.
[16] S. Hamoudi, Y. Yang, I.L. Moudrakovski, S. Lang, A. Sayari, J. Phys. Chem. B 105 (2001) 9118.
[17] H. Fan, Y. Lu, A. Stump, S.T. Reed, T. Baer, R. Schunk, V. Perez-Luna, G.P. Lopez, C.J. Brinker, Nature 405 (2000) 56.
[18] Y. Lu, H. Fan, N. Doke, D.A. Loy, R.A. Assink, D.A. LaVan, C.J. Brinker, J. Am. Chem. Soc. 122 (2000) 5258.
[19] K.J. Shea, D.A. Loy, Chem. Mater. 1 (1989) 572.
[20] K.J. Shea, D.A. Loy, O. Webster, J. Am. Chem. Soc. 114 (1992) 6700.
[21] K.J. Shea, D.A. Loy, Chem. Rev. 95 (1995) 1431.
[22] R.J.P. Corriu, D. Leclerq, Angew. Chem. Int. Ed. 35 (1996) 1420.
[23] G. Cerveau, R.J.P. Corriu, Coord. Chem. Rev. 178–180 (1998) 1051.
[24] R.J.P. Corriu, Angew. Chem. Int. Ed. 39 (2000) 1376.
[25] M.C. Burleigh, M.A. Markowtiz, M.S. Spector, B.P. Gaber reported that base-catalyzed polymerization of bis [3-trimethoxysilyl)propyl]ethylenediamine has been achieved using cetyltrimethylammonium chloride (CTAC) as the surfactant template as an unpublished results in Ref. [27] (Chem. Mater. 13 (2001) 4760).
[26] K.Z. Hossain, L. Mercier, Adv. Mater. 14 (2002) 1053.
[27] M.C. Burleigh, M.A. Markowtiz, M.S. Spector, B.P. Gaber, Chem. Mater. 13 (2001) 4760.
[28] C.E. Flower, S.L. Burkett, S. Mann, Chem. Commun. (1997) 1769.
[29] S.L. Burkett, S.D. Sims, S. Mann, Chem. Commun. (1997) 1769.

[30] B. Park, J. Park, W. Guo, I. Kim, C.S. Ha, Micropor. Mesopor. Mater. 66 (2003) 229.
[31] D. Margolese, J.A. Melero, C.S. Cristiansen, B.F. Chemelka, G.D. Stucky, Chem. Mater. 12 (2000) 2448.
[32] M.C. Burleigh, S. Dai, E.W. Hagaman, Chem. Mater. 13 (2001) 2537.
[33] M.A. Wahab, W. Guo, W.J. Cho, C.S. Ha, J. Sol-Gel Sci. Technol. 27 (2003) 333.
[34] C.T. Kresege, M.E. Leonovica, M.E. Roth, W.J. Vartuli, W.C. Vartuli, US Patent No. 5098684, 1992.
[35] P.T. Tanev, M. Chibwe, P.T. Pinnavaia, Nature 368 (1994) 321.
[36] T. Asefa, M. Kruk, M.J. MacLachlan, N. Coombs, H. Grondey, M. Jaroniec, G.A. Ozin, J. Am. Chem. Soc. 123 (2001) 8520.
[37] S.L. Butkett, S.D. Sims, S. Mann, Chem. Commun. (1996) 1367.
[38] Y. Mori, T.J. Pinnavaia, Chem. Mater. 13 (2001) 2173.
[39] A. Stein, B.J. Melde, R.C. Schroden, Adv. Mater. 12 (2000) 1403.
[40] M.H. Lim, C.F. Blanford, A. Stein, Chem. Mater. 11 (1999) 3285.
[41] T. Salesch, S. Bachmann, S. Brigger, R.R. Schaefer, K. Albert, S. Steinbrecher, E. Plies, A. Mehdi, C. Reye, R.J.P. Corriu, E. Linder, Adv. Func. Mater. 12 (2002) 134.
[42] K.S.W. Sing, D.H. Evernett, R.A.W. Haul, L. Moscou, P.A. Pierotti, J. Rouquerol, T. Siemieniewska, Pure Appl. Chem. 57 (1985) 603.
[43] T. Asefa, M.J. MacLachlan, N. Coombs, G.A. Ozin, Nature 402 (1999) 867.
[44] M.P. Kapoor, S. Inagaki, Chem. Mater. 14 (2002) 3509.
[45] H. Zhu, D.J. Jones, J. Zajac, R. Dutarture, M. Rhomari, J. Roziere, Chem. Mater. 14 (2002) 4886.
[46] D.L. Vien, W.B. Colthup, W.G. Fately, J.G. Grasseli, The Handbook of Infrared and Raman Characteristic Frequency of Organic Molecules, Academic Press, New York, 1991, p. 43; W.B. Colthup, L.H. Daly, S.E. Wiberley, Introduction to Infrared and Raman Spectroscopy, 3rd Edition, Academic Press, New York, 1990.
[47] N. Liu, R.A. Assink, B. Smarsly, C.J. Brinker, Chem. Commun. (2003) 1146.
[48] V. Antochshuk, M. Jaroniec, Chem. Commun. (2002) 258.
[49] T. Yokoi, H. Yoshitake, T. Tatsumi, Chem. Mater. 15 (2003) 4536.
[50] S. Huh, J.W. Wiench, J.C. Yoo, M. Pruski, V.S.Y. Lin, Chem. Mater. 15 (2003) 4247.
[51] D.A. Loy, G.M. Jamison, B.M. Baugher, E.M. Russick, R.A. Assink, S. Prabaker, K.J. Shea, J. Non-Cryst. Solids 44–53 (1995) 186.
[52] A.M. Liu, K. Hidajat, S. Kawi, D.Y. Zhao, Chem. Commun. (2000) 1145.
[53] T. Asefa, M. Kruk, N. Coombs, H. Grondey, M.J. Maclachlan, M. Jaroniec, G.A. Ozin, J. Am. Chem. Soc. 125 (2003) 11662.
[54] M.A. Markowitz, J. Klaehn, R.A. Hendel, S.B. Qadriq, S.L. Golledge, D.G. Castner, B.A. Gaber, J. Phys. Chem. B 104 (2000) 10820.
[55] J.F. Moulder, W.F. Stickle, P.E. Sobol, K.D. Bomben, Handbook of X-ray Photoelectron Spectroscopy, Physical Electronics, Inc. USA, October 1995.
[56] P.K. Brow, C.G. Pantano, J. Am. Ceram. Soc. 70 (1987) 9.